

Performance studies of resistive Micromegas chambers for the upgrade of the ATLAS Muon Spectrometer

Konstantinos Ntekas^{1,2,a} on behalf of the ATLAS Muon Collaboration

¹National Technical University of Athens, Zografou Campus, 9, GR-159 73 Athens, Greece

²Brookhaven National Laboratory, Building 510, Upton NY 11973, US

Abstract. The ATLAS collaboration at LHC has endorsed the resistive Micromegas technology (MM), along with the small-strip Thin Gap Chambers (sTGC), for the high luminosity upgrade of the first muon station in the high-rapidity region, the so called New Small Wheel (NSW) project. The NSW requires fully efficient MM chambers, up to a particle rate of $\sim 15 \text{ kHz/cm}^2$, with spatial resolution better than $100 \mu\text{m}$ independent of the track incidence angle and the magnetic field ($B \leq 0.3 \text{ T}$). Along with the precise tracking the MM should be able to provide a trigger signal, complementary to the sTGC, thus a decent timing resolution is required. Several tests have been performed on small ($10 \times 10 \text{ cm}^2$) MM chambers using medium (10 GeV/c) and high (150 GeV/c) momentum hadron beams at CERN. Results on the efficiency and position resolution measured during these tests are presented demonstrating the excellent characteristics of the MM that fulfil the NSW requirements. Exploiting the ability of the MM to work as a Time Projection Chamber a novel method, called the μTPC , has been developed for the case of inclined tracks, allowing for a precise segment reconstruction using a single detection plane. A detailed description of the method along with thorough studies towards refining the method's performance are shown. Finally, during 2014 the first MM quadruplet (MMSW) following the NSW design scheme, comprising four detection planes in a stereo readout configuration, has been realised at CERN. Test-beam results of this prototype are discussed and compared to theoretical expectations.

1 The ATLAS New Small Wheel Upgrade Project (NSW)

The upgrade of the ATLAS [1] muon spectrometer is primarily motivated by the high background radiation expected during Run 3 (2020) and ultimately at $\mathcal{L} = 7 \times 10^{34} \text{ cm}^{-2}\text{s}^{-1}$ in HL-LHC (2025). Owing to this the detectors that occupy the innermost muon station called Small Wheel (SW), MDT, CSC & TGC, will go beyond their design luminosity limit of $\mathcal{L} = 1 \times 10^{34} \text{ cm}^{-2}\text{s}^{-1}$. In addition, the muon trigger rate will exceed the available bandwidth because of the fake endcap muon triggers (90% is coming from low energy particles, generated in the material located between the Small Wheel and the outer endcap muon station). The collaboration has decided to replace the SW with a NSW system [2], shown in Fig. 1, combining sTGC [3] & resistive MM detectors [4, 5]. Both detector technologies should provide tracking and triggering information for redundancy. The NSW will contribute to the suppression of fake triggers by reconstructing high quality ($\sigma_\theta \sim 1 \text{ mrad}$) IP pointing segments online. Moreover, efficient & precise offline tracking ($\sigma_r \leq 100 \mu\text{m}$) even for the maximum expected rate of 15 kHz/cm^2 is required.

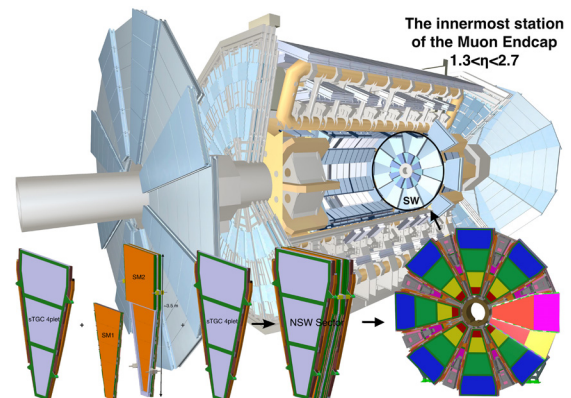


Figure 1. The muon system of the ATLAS experiment. The NSW will combine eight MM and eight sTGC detection layers per sector (eight small and eight large sectors per wheel).

2 Performance studies using test beams

In order to demonstrate the excellent performance of the MM technology and also optimise the design and operational parameters of the detector, several small and medium size chambers have been tested with medium and high momentum hadron beams at CERN. A graphical representation of the resistive MM internal structure and principle of operation is shown in Fig. 2. For the results that

^ae-mail: konstantinos.ntekas@cern.ch

are presented, the front-end electronics were based on the APV25 ASIC (128 channels) [6], which will not be employed in the NSW, readout through the Scalable Readout System (SRS) developed by the RD51 collaboration [7]. The front-end ASIC providing the trigger and tracking primitives for both the MM and sTGC of the NSW will be the VMM [8] currently being produced in its second prototype version.

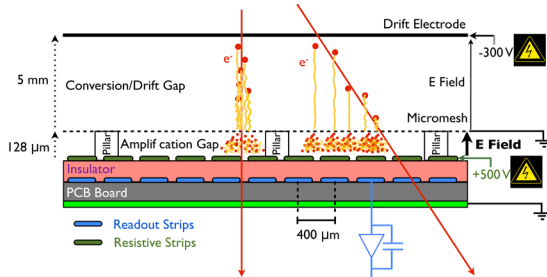


Figure 2. Cross-section of the resistive MM internal structure. A layer of resistive strips matching the read-out pattern makes the detector insensitive to discharges coming from massive ionisations.

3 Hit & Track reconstruction

The APV25 chip samples the charge every 25 ns over a predefined range (≤ 675 ns). By analyzing the evolution of the integrated charge on each strip, as described in Fig. 3, the arrival time of each primary cluster along with the charge amplitude is calculated. Utilising the measured charge and time information, two different hit reconstruction techniques have been developed:

- **(Charge) Centroid** : Average of the strip position weighted by the strip charge.
- **μ TPC** : 2D track reconstruction transforming the arrival time into distance. The hit is defined by the track interpolation in the middle of the drift gap. The track angle is measured using the slope of the reconstructed segment.

The charge centroid method reconstructs hits with high accuracy when the particle traverses the chamber plane perpendicularly. In this case the charge is shared among only a few strips allowing for a very precise charge interpolation. The spatial resolution determined with this method is well below $100 \mu\text{m}$ for perpendicular tracks. The μ TPC method does not provide accurate results in this case as the pulse in each strip is the aggregation of pulses induced by more than one primary ionisation clusters generated at different heights within the drift gap. When a charged particle crosses the detector under an angle, the primary ionisation charge is distributed along several readout strips, with the signal induced in each strip is most probably coming from one primary cluster. In this occasion the μ TPC method provides a very accurate measurement of the particle hit position on the detector. However, the strip signal amplitude becomes sensitive to the primary cluster charge fluctuations and thus the accuracy of the charge centroid

method deteriorates with increasing track inclination angles.

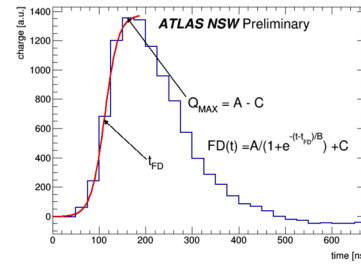


Figure 3. The integrated charge time evolution in a single strip over 25 samples of 25 ns each. A Fermi-Dirac function is used to describe the rising edge of the distribution and extract the time t_{FD} and the charge amplitude Q_{MAX} . (Taken from Ref. [9])

3.1 Refinement of the μ TPC method

In the NSW the MM will be exposed to particle track angles between 8° and 30° . Thus, the performance of the μ TPC track reconstruction method is of great importance for the ATLAS NSW MM project and a lot of effort has been dedicated in optimising the performance of this technique. An advanced clustering algorithm has been developed that properly treats events with more than one track, or events with noise and/or delta rays ($\sim 10\%$ of the events). A pattern recognition, using the Hough transform, is used for the track identification increasing the efficiency of the event selection and improving the accuracy of the reconstructed track by removing outlying strips [10].

Moreover, owing to the readout elements geometry, there is a non-negligible capacitance between adjacent strips causing the ionization charge to be shared among the neighbouring readout elements. The effect has been studied in simulation concluding that $\sim 10\%$ of the charge induced on a strip is capacitively coupled to its neighbours. This may bias the reconstructed track by artificially increasing the track footprint. A filtering algorithm has been developed identifying strips with charge coupled only from their neighbours discarding them from the track reconstruction procedure.

Another parameter that should be finely tuned is the assignment of the hit position along the strip pitch. In the offline reconstruction each strip position is usually assigned in the middle of the strip pitch. Actually, this is correct only for the middle strips of the cluster where the hit position is uniformly distributed along the strip pitch. For the edges of the cluster it is more probable for the hit position to be towards the strip pitch edge neighbouring to the cluster strips. The assignment of the hit in the middle of the strip pitch for the cluster edges results in biasing the reconstructed track towards larger inclination values, thus a method has been developed tuning the hit position on the cluster edges [11].

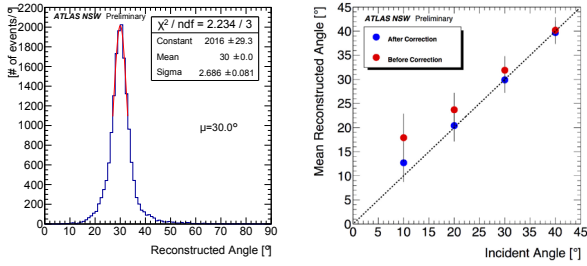


Figure 4. Left: Distribution of the track angle reconstructed with the μ TPC method for a MM chamber inclined by 30° with respect to the beam. Right: The peak reconstructed angle as a function of the track inclination angle before and after the refinement of the μ TPC method. (Taken from Ref. [9])

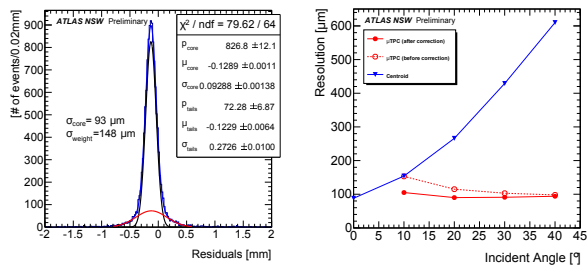


Figure 5. Left: Distribution of the position difference, divided by $\sqrt{2}$, between the reconstructed μ TPC hits of two MM chambers inclined by 30° with respect to the beam. Right: The measured single spatial resolution for the centroid and the μ TPC method, before and after the refinement, are shown as a function of the track angle. (Taken from Ref. [9])

The refined μ TPC reconstruction algorithm was applied in test beam data with small size ($10 \times 10 \text{ cm}^2$) prototypes exposed to a 120 GeV/c π^+ beam at CERN under different inclination angles. The reconstructed track angle and the measured spatial resolution with and without the refined algorithm are compared. The improvement in the accuracy of the μ TPC method, using the techniques described above, is not only evident in the better agreement of the measured incident angle with the true one shown in Fig. 4, but also in the measurement of the spatial resolution which is displayed in Fig. 5. The impact is more significant for smaller incident angle values.

4 The effect of pillars in hit reconstruction

In addition to the precise hit position reconstruction the NSW MM detectors should be fully efficient even at the highest rates of 15 kHz/cm^2 that are expected after the LHC upgrade. Along these lines, the efficiency of the small MM chambers has been studied in test beams in order to fully characterise and understand possible contributions to the detector inefficiency. Results for chambers with different characteristics and with different track inclination angles are presented.

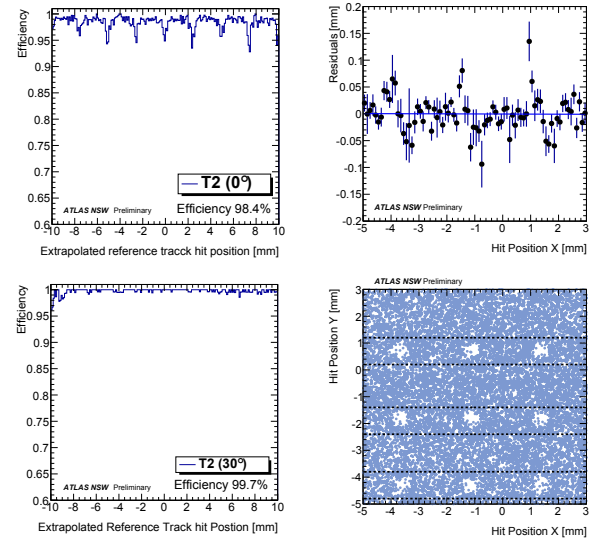


Figure 6. Left: The $300 \mu\text{m}$ in diameter cylindrical pillars placed every 2.5 mm supporting the mesh contribute 1.5% inefficiency in the case of perpendicular tracks. For inclined tracks the pillars are transparent to the efficiency owing to the larger number of strips fired per track. Right: Owing to the distortion of the electric field lines the reconstructed hit position is biased in the the pillar region by as much as $150 \mu\text{m}$. (Taken from Ref. [9])

The efficiency is calculated by comparing the hits reconstructed in a single chamber with the reference chambers of the experimental set-up. The measured efficiency is plotted as a function of the reference track hit position for a MM chamber with a single readout layer in Fig. 6 (left column). In the top left plot, the case where the chamber plane is positioned vertically with respect to the beam axis is shown. Local efficiency drops, up to 5% , owing to the pillars appear every 2.5 mm . The total measured efficiency is rather high with only $\sim 1.6\%$ geometrical inefficiency attributed to the pillars. However, when the chamber is inclined by 30° with respect to the beam the pillars are no longer visible as shown in Fig. 6 (bottom left). The larger track footprint for inclined tracks makes the efficiency measurement insensitive to the pillars and an efficiency close to $\sim 100\%$ is reached.

Apart from affecting the MM efficiency, the presence of pillars locally distorts the electric field lines [12] biasing the reconstructed hit position in their vicinity. The effect has been measured for perpendicular tracks in a test beam, by calculating the residuals between a reference track and the reconstructed hit as a function of the reconstructed hit position. A MM chamber with 2D readout [13] was used and only hits reconstructed across "bands of pillars", as shown in Fig. 6 (bottom right), were included in the analysis. A bias in the reconstructed hit position around each pillar is evident in Fig. 6 (top right) with a maximum deviation of $\sim 150 \mu\text{m}$ which is in qualitative agreement with what has been measured in simulation studies of a MM with different operational parameters [12].

5 Performance study of the first MM quadruplet

The performance of the recently developed MM quadruplet (MMSW) [14] was studied in a dedicated test beam at CERN. The MMSW was positioned in the beam line along with a hodoscope equipped with small MM chambers providing the 2D reference track. The operation of the MMSW, using the standard Ar+7%CO₂ gas mixture, was smooth during the whole period of irradiation with all the four layers being ~ 99% efficient. For the results presented here the chamber was kept perpendicular to the beam axis.

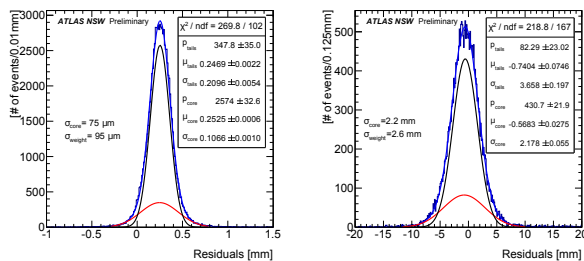


Figure 7. Left: Distribution of the hit position difference, divided by $\sqrt{2}$, between the precision coordinate layers of the MMSW. Right: Residual distribution of the MMSW second coordinate hit position with a second coordinate hit coming from one of the reference chambers. (Taken from Ref. [9])

By plotting the hit position difference between the first two layers of the MMSW, with readout strips parallel to each other, we were able to determine the spatial resolution of each of the two precision layers equal to 75 μm as shown in Fig. 7 (left). Exploiting the stereo readout strip geometry of the quadruplet, the second coordinate is also reconstructed. The chambers of the reference telescope are used to reconstruct the second coordinate of the extrapolated track on the MMSW frame. By comparing this with the second coordinate hit reconstructed combining the information from two stereo readouts the spatial resolution of the second coordinate is measured to be of the level of 2.2 mm, Fig. 7 (right) which is in accordance with theoretical expectations. Simulation studies of the stereo strips configuration [15] dictate, that by combining two stereo layers, with a 3° angle between them, the second coordinate can be reconstructed with an uncertainty of ~ 2.2 mm, assuming single layer spatial resolution of ~ 80 μm .

6 Conclusions

A series of performance studies in order to optimise the MM performance and operating conditions, in the context

of the ATLAS NSW upgrade, are presented. The studies are mainly focussed on the development and optimisation of the μTPC reconstruction method that provides a precise segment reconstruction using a single detector gap. Moreover, studies on the contribution of the pillars in the measured efficiency and hit reconstruction accuracy are discussed. A non-negligible effect is measured for perpendicular tracks which is in qualitative agreement with simulation calculations. Finally, the MMSW quadruplet prototype, that follows the final NSW MM quadruplet layout, has been studied in test beam and the results presented follow the simulation and theoretical expectations.

Acknowledgements

The work was co-funded by the European Union (European Social Fund ESF) and Greek national funds through the Operational Program "Education and Lifelong Learning" of the National Strategic Reference Framework (NSRF) 2007-2013 ARISTEIA-1893-ATLAS MICROMEGAS.

References

- [1] ATLAS Collaboration, JINST 3 S08003 (2008)
- [2] ATLAS Collaboration, CERN-LHCC-2013-006, ATLAS-TDR-020 (2013)
- [3] V. Smakhtin *et al.*, Nucl. Instr. Meth. A 598 196-200 (2009)
- [4] Y. Giomataris *et al.*, Nucl. Instr. Meth. A376, 29-35, (1996)
- [5] T. Alexopoulos *et al.*, Nucl. Instr. Meth. A 640 110-118 (2011)
- [6] M.J. French *et al.*, Nucl. Instr. Meth. A466, 359-365, (2001)
- [7] S. Martoiu *et al.*, Nucl. Sc. Symp. and Med. Imag. Conf., IEEE, pp.2036,2038 (2011)
- [8] G. De Geronimo *et al.*, IEEE Transactions on Nuclear Science, vol. 60, no. 3, (2013)
- [9] ATLAS NSW Public Results : <https://twiki.cern.ch/twiki/bin/view/AtlasPublic/NSWPublicResults>
- [10] T. Alexopoulos *et al.*, ATL-UPGRADE-PUB-2014-001 (2014)
- [11] K Ntekas, ATL-MUON-PROC-2014-011 (2014)
- [12] P. Bhattacharya *et al.*, Nucl. Instr. Meth. A 793, 41-48 (2015)
- [13] M. Byszewski *et al.*, Journal of Instrumentation 7 02, C02060 (2015)
- [14] M. Bianco *et al.*, arXiv:1511.03884 (2015)
- [15] T. Alexopoulos *et al.*, ATL-MUON-PUB-2015-001 (2015)